

# Evaluation of Critical Stress Intensity Factor for Different RSW Joints

## Ismail Benchadli

Mechanical Systems and Materials Engineering Laboratory, Mechanical Engineering Department, Faculty of Technology, University of Tlemcen, Algeria  
Ismailtreez15@gmail.com

## Mustapha Benachour

Mechanical Systems and Materials Engineering Laboratory, Mechanical Engineering Department, Faculty of Technology, University of Tlemcen, Algeria  
bmf\_12002@yahoo.fr (corresponding author)

## Fethi Sebaa

Mechanical Systems and Materials Engineering Laboratory, Mechanical Engineering Department, Faculty of Technology, University of Tlemcen, Algeria  
sebaafethi@yahoo.fr

## Nadjia Benachour

Mechanical Systems and Materials Engineering Laboratory, Physics Department, University of Tlemcen, Algeria  
nbenachour2005@yahoo.fr

Received: 8 June 2024 | Revised: 13 July 2024 | Accepted: 16 July 2024

Licensed under a CC-BY 4.0 license | Copyright (c) by the authors | DOI: <https://doi.org/10.48084/etasr.8030>

## ABSTRACT

The aim of this paper is to evaluate the critical stress intensity factor (fracture toughness) for a range of Resistance Spot Welding (RSW) joints. The geometry of resistance spot welding joints under investigation comprises lap joints and coach peel joints of 316L stainless steel. The critical stress intensity factor of RSW lap joints and coach peel joints is calculated based on the experimental results of the shearing tensile tests and peel tensile tests, respectively. The welding parameters under investigation are the welding current, welding time, and electrode force. This study employs a fracture mechanics-based approach, to investigate the influence of RSW welding parameters on the critical stress intensity factor. The results demonstrate that the critical stress intensity factor exhibits a relatively decreasing trend with an increase in the welding current, from 8 kA to 16 kA. Moreover, an increase in the nugget diameter is particularly influenced by an increase in the welding current.

*Keywords-Resistance Spot Welding (RSW); welding parameters; coach peel joints; fracture toughness; stainless steel*

## I. INTRODUCTION

A variety of welding processes have been employed in manufacturing industries, including Gas Tungsten Arc Welding (GTAW), Submerged Arc Welding (SAW), Shielded Metal Arc Welding (SMAW), Resistance Spot Welding (RSW), and Fast Stir Welding (FSW). RSW is a welding process that is widely used in manufacturing due to its high degree of repeatability, low-cost equipment, and straightforward process control [1], for joining different metals, particularly stainless steels [2-5]. The employment of stainless steels has become prevalent in a multitude of industrial contexts, largely due to

their advantageous corrosion resistance, mechanical properties, and aesthetic appeal in the context of welding. The evaluation of fracture toughness in resistance spot-welded lap joints or resistance spot-welded coach peel joints is a means of establishing high resistance fracture. Authors in [6] evaluated the fracture toughness of resistance spot-welded lap joints of galvanized steel sheets from the stress intensity factor in mode II. The experimental results demonstrate that an increase in the welding current, leads to an enhancement in the fracture toughness. Based on a stress analysis around the spot weld in lap joints and coach peel joints of Pook Works, authors in [7] have determined expressions for the variation of stress intensity

factors in modes I and II. In the context of an overlap joint subjected to mixed loading conditions, authors in [10] have proposed the use of an equivalent stress intensity factor as a means of evaluating the fracture toughness. Authors in [11] have employed the stress intensity factor solutions proposed by [7, 8], to predict fatigue using the law in [12]. The stress intensity factor solutions for spot welds in coach-peel specimens were investigated through the use of finite element analyses. Three-dimensional finite element models were constructed in order to obtain accurate stress intensity factor solutions [13]. The numerical results indicated the presence of three modes of fracture, with mode I being the predominant one. Authors in [14] examined the influence of temperature on plain fracture toughness in representative regions of a low-alloyed Cr-Mo steel A-387 Gr-B welded joint.

The effects of weld nugget size on the critical stress intensity factor of martensitic stainless steel resistance spot welds are investigated by authors in [15]. The findings indicate that the fracture toughness is not contingent upon the dimensions of the weld nugget. Authors in [16] have devised a novel methodology for measuring the fracture toughness at the onset of cracking and the crack extension resistance of the molten zone of resistance spot welds under Mode I loading, deploying U-shaped specimens. The results indicate that the fracture toughness at crack initiation of the nugget is independent of the base material's mechanical properties and the nugget diameter. The objective of this study is to investigate the effect of welding parameters of RSW using two RSW geometries, namely tensile shear joints and coach peel joints, on the critical stress intensity factor and the size of the nugget in 316L stainless steel. Analytical models for various geometries [17, 18], are employed to assess the critical stress intensity factor.

## II. EXPERIMENTAL PROCEDURE

The base metal was selected to be a stainless steel 316L sheet with a thickness of 1.5 mm, with a chemical composition which is presented in Table I, and mechanical properties which are shown in Table II. Welding experiments were conducted using the resistance spot welding process. Tensile shear joints and coach peel joints, evidenced in Figure 1, were utilized for tensile mechanical testing. The spot welds were conducted using a machine (TECNA) equipped with a pneumatic pressure system. The welding current and time were input manually and it was assumed that the diameter of the electrode tip remained constant at 7 mm. The welding time, current, and electrode force represent variable welding parameters. The selected values of the welding current range from 8 kA to 16 kA, while the welding times are 10, 11, and 13 cycles. The chosen values of the electrode force are 6 bar and 8 bar. The number of specimens to be welded was determined through the use of factorial analysis. The tensile shear and coach peel tests were carried out on the ControLab testing machine with a capacity of 600 kN and with a constant speed of 30 mm/min. The experimental data are presented in the shape load-displacement diagrams used to ascertain the fracture force of the welded specimens. Additionally, the diameters of the welding nuggets are gauged in accordance with the American Welding Society (AWS) standards [19], as observed in Figure 2. These

measurements are then employed to ascertain the fracture toughness of the tensile shear joints and coach peel joints. The button size is determined by means of a knife-edge dial caliper.

TABLE I. CHEMICAL COMPOSITION OF THE 316L STAINLESS STEEL

C	Cr	Mn	Mo	N
0.03	16.5-18.5	2	2-2.5	0.1
P	Ni	Si	S	
0.045	10.0-13.0	1	0.015	

TABLE II. MECHANICAL PROPERTIES OF 316L STAINLESS STEEL

$\sigma_{0.2\%}$ (MPa)	UTS (MPa)	A%	$\nu$
315.59	627.86	51.17	0.30

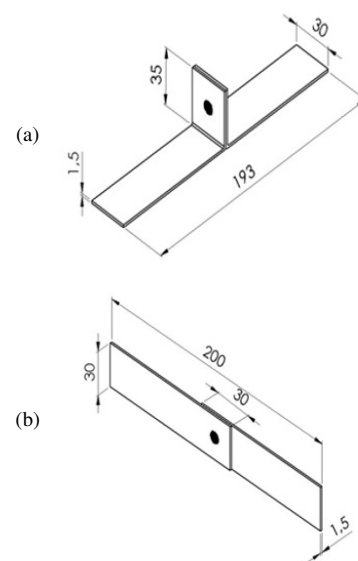


Fig. 1. Experimental specimens: (a) coach peel joint (b) tensile shear joint.

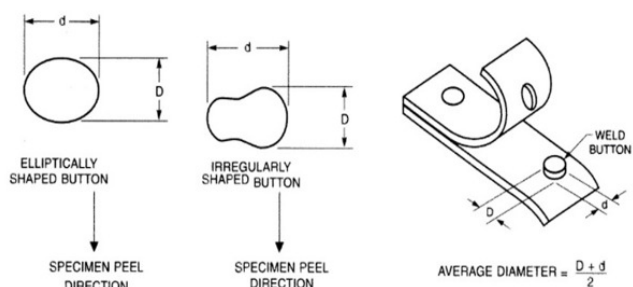


Fig. 2. Welding nugget measurement AWS standards.

## III. BACKGROUND ON EVALUATION OF FRACTURE TOUGHNESS

Authors in [20] provided a crucial insight into the calculation of stress intensity parameters in the presence of a fissure between two sheets subjected to edge loads. Subsequently, authors in [9] demonstrated the validity of this solution, which involves multiplying the structural stress at the crack's point by the square root of the metal sheet thickness. The simplified plate theory could be employed to directly

calculate the stress concentrations at the crack tip. This study introduces an innovative approach for determining stress intensity values for spot welds, which is based on the concept of structural stress. The concept of structural stress was further examined by authors in [21], in [7, 17, 22], and authors in [23-28], contributed to a number of formulations that employed structural stress as an input parameter for determining stress intensity parameters in spot welds. The primary objective of their investigation was to ascertain the fatigue strength of resistance spot welds. In the present study, the stress intensity factors under various loading conditions for two distinct types of joints were calculated.

A. Tensile Shear Joint

The most significant stress-inducing variables at the front-facing vertex parallel to the loaded direction (at the point A in Figure 3), *KI* and *KIII*, occur concurrently and can be determined as [7, 17, 22]:

$$KI = \frac{F\sqrt{3}}{2\pi D\sqrt{t}} \tag{1}$$

$$KII = \frac{F}{\pi D\sqrt{t}} \tag{2}$$

The following equation can be employed to ascertain the maximum *KIII* at the nugget edge's side facing vertex (at the point B in Figure 3) for tensile-shear spot welds:

$$KIII = \frac{F\sqrt{2}}{\pi D\sqrt{t}} \tag{3}$$

In fact, the equivalent stress intensity factor is given as:

$$Keqc = \frac{F\sqrt{19}}{2\pi D\sqrt{t}} \tag{4}$$

where *KI*, *KII* and *KIII* are the stress intensity factors in MPa/m<sup>2</sup>, *Keqc* is the equivalent stress intensity factor in MPa/m<sup>2</sup>, *D* is the diameter of the nugget (mm), *t* is the thickness of the plate (mm), and *F* is the applied force in the tensile shear RSW.

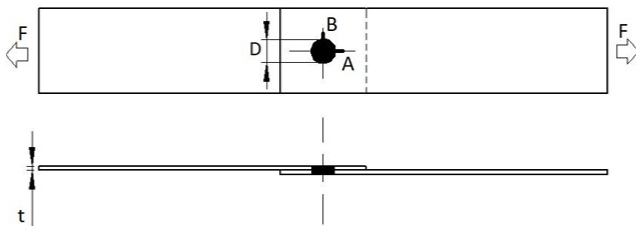


Fig. 3. Tensile shear joint under load *F*.

B. Coach Peel Joint

Based on the symmetry, the highest stress intensity factors for the coach-peel spot welding are found to coincide (point A, in Figure 4) and are determined as [7, 17, 22]:

$$KI = \frac{3\sqrt{2}eP}{\pi D\sqrt{t}} \quad (KII = KIII = 0) \tag{5}$$

with the coach peel joint's equivalent stress intensity factor being:

$$Keqc = \frac{2\sqrt{3}eP}{\pi D\sqrt{t}} \tag{6}$$

where *e* is the distance from center of the nugget to the applied force (mm) and *P* is the applied force in the coach peel joint.

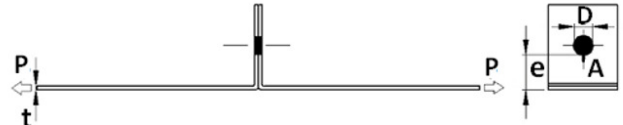


Fig. 4. Coach-peel joint under load *P*.

IV. RESULTS AND DISCUSSION

A. Effect of Welding Parameters on Mechanical Properties

The evolution of load-displacement curves under variation of the welding current is presented in Figure 5, for tensile shear joints and coach peel joints. In the case of a tensile shear joint, an increase in the welding current results in an increase in the displacement and maximum load. For a welding current of 16 kA, a reduction in the displacement and a negligible reduction in the maximum load were observed in comparison to the maximum load for a welding current of 14 kA. In the case of the coach peel joint, a reduction in the maximum load is evidenced in comparison to the maximum load detected in the tensile shear joint. In the coach peel joint, the load-displacement curves are divided into two distinct zones. The initial zone contains the load-displacement curves corresponding to the RSW points, while the subsequent zone includes the load-displacement curves noted in the base metal, which illustrate the tearing of the base metal. As evidenced by the load-displacement curves, an increase in maximum load was observed with an increase in the welding current, under fixed weld time and applied electrode force conditions. Additionally, an increase in displacement was observed for a constant load in Zone II as the welding current was reduced. A high maximum load is observed for a welding current of 16 kA, with no displacement occurring in conjunction with this welding current. This indicates that no tearing of the base metal occurs under these conditions.

B. Effect of Welding Current on Geometrical Parameters

Figure 6 displays the evolution of the nugget size under the influence of welding current and welding time for a fixed electrode force for tensile shear joints and coach-peel joints. An increase in the welding current results in a corresponding increase in the nugget diameter, as a consequence of enhanced heat transfer. Furthermore, the effect of welding time on nugget diameter is found to be insignificant. The influence of the welding current on the nugget diameter remains consistent when electrode force is maintained at 8 bars. Thus, it can be observed that there is a slight influence of the welding time on the variation of nugget diameter. At a welding current of 12 kA, an increase of 0.4 mm was observed in the nugget diameter with an increase in the welding time from 10 to 13 cycles. Furthermore, there is a slight reduction in the nugget diameter with an increase in electrode force.

C. Effect of Welding Current on Penetration Depth in RSW Point

The evolution of the penetration depth in resistance spot welding is shown in Figure 7 for electrode forces of 6 bar and 8

bar. It was observed that an increase in the penetration depth occurred in accordance with an increase in the welding current [33]. Furthermore, the impact of welding time is inconsequential for welding currents between 10 kA and 14 kA for  $F=6$  bar and 8 bar. Consequently, for a welding time of 10 cycles and  $F=6$  bar, a minimal discrepancy in penetration depth is discernible in comparison to other welding times. For electrode force  $F=8$  bar, no effect of welding time is observed for all variations of the welding current.

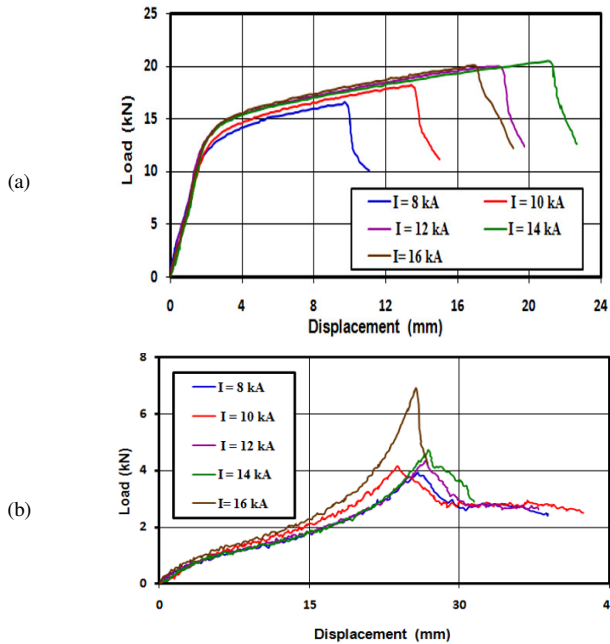


Fig. 5. (a) Load/Displacement curves under the effect of welding current for tensile shear joint for  $T=11$  cycles and  $F=6$  bar, (b) load/displacement curves under the effect of welding current for Coach Peel joints.

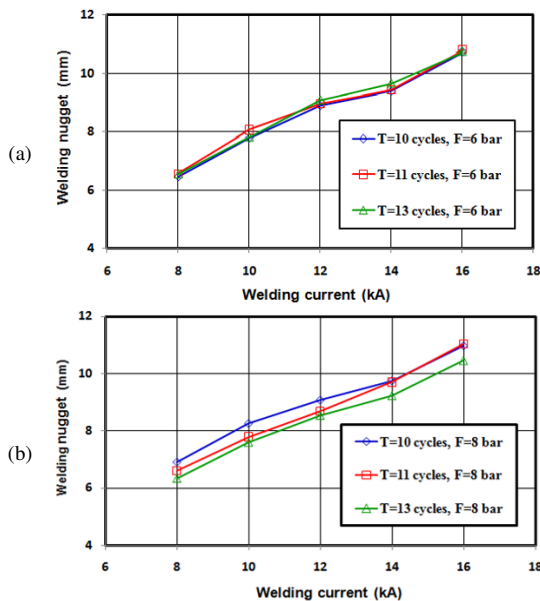


Fig. 6. (a) Welding current effect on nugget size for  $F=6$  bar, (b) welding current effect on nugget size for  $F=8$  bar.

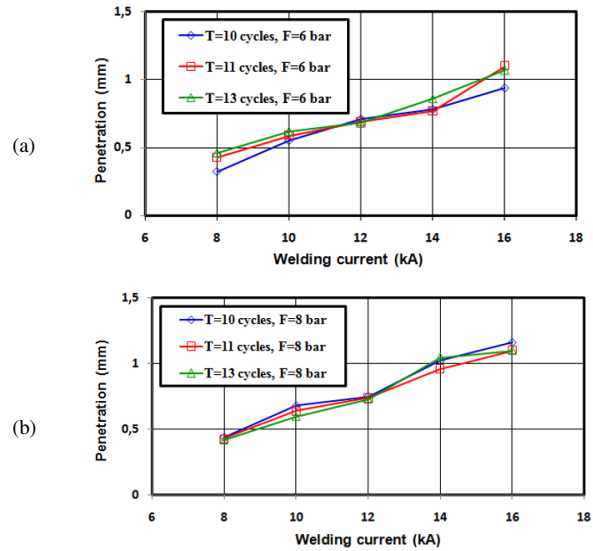


Fig. 7. (a) Welding current effect penetration depth for  $F=6$  bar, (b) welding current effect on penetration depth for  $F=8$  bar.

#### D. Effect of Welding Current on Fracture Toughness

As exhibited in Figure 8, an increase in the welding current results in a reduction in fracture toughness. Authors in [6], verified that within the identical range of welding currents, there is a spanning from 8 kA to 10 kA. This phenomenon can be attributed to the high melting and splashing that occurs at the specified welding current. In comparison to other welding currents, a tensile shear joint with an 8-kA current demonstrates comparatively high fracture toughness. Additionally, minimal fracture toughness is detected at 16 kA. An increase in welding time has a gradual negative effect on fracture toughness, with the exception of welding times equal to 13 cycles. In the coach peel joint, a dispersion of the effect of the welding current on fracture toughness is demonstrated for all welding times and all electrode forces. Additionally, it was observed that for a low welding current ( $I=8$  kA), the fracture toughness is at its maximum in comparison to other welding currents, and then decreases with the increase of the welding time and electrode force.

Figure 9 presents an increase in the welding current results along with a reduction in fracture toughness from 8 kA to 12 kA for the coach peel joint. A slight variation in fracture toughness is observed for  $F=6$  bar when the welding current is increased from 12 kA to 16 kA. Furthermore, disparities are evident in the correlation between welding current and welding time for  $F=8$  bar. These developments are attributable to both the duration of the welding process and the formation of the weld nugget, as well as the hardness at the boundary between the nugget and the Heat-Affected Zone (HAZ) [34].

#### V. CONCLUSIONS

The distinctive quality of this work lies in its integration of experimental findings on the impact of spot-welding parameters with analytical techniques for assessing the critical stress intensity factor. Furthermore, standardized procedures

were employed to ascertain the mean weld nugget diameter for each welding current utilized in the analytical models.

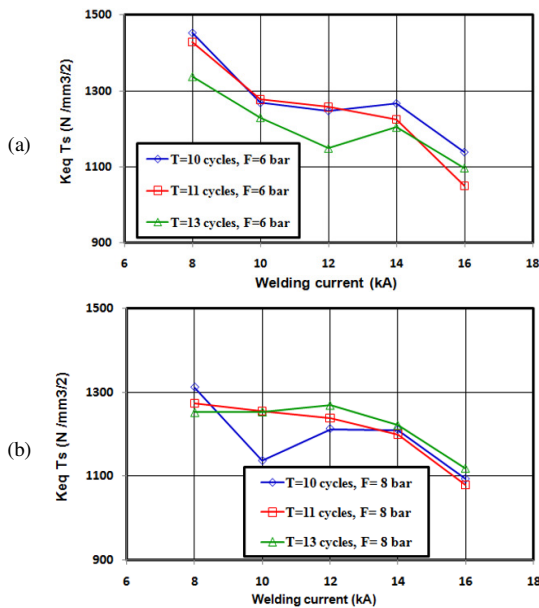


Fig. 8. (a) Effect of welding current on  $Keqc$  of tensile shear joint for  $F=6$  bar, (b) Effect of welding current on  $Keqc$  of tensile shear joint for  $F=8$  bar.

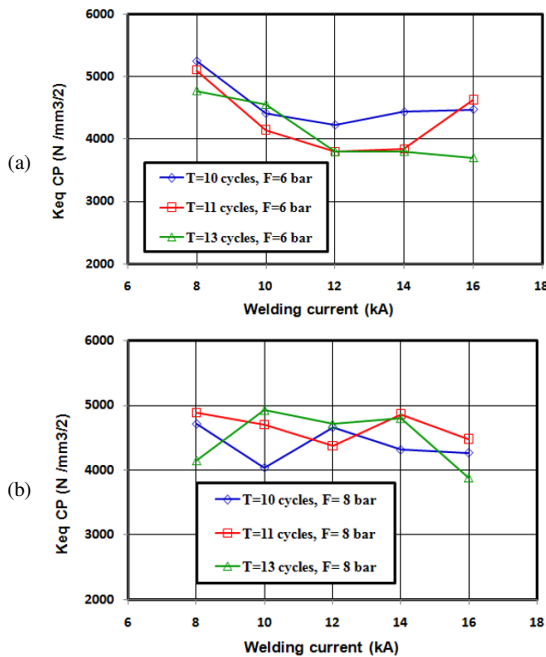


Fig. 9. (a) Effect of welding current on  $Keqc$  of coach peel joints for  $F=6$  bar, effect of welding current on  $Keqc$  of coach peel joints for  $F=8$  bar.

The investigation into resistance spot welding joints reveals a complex relationship between welding parameters and mechanical properties, which is influenced by a number of factors, including welding current, welding time, electrode force, and critical stress intensity factor (fracture toughness). Higher welding currents typically result in increased

penetration depth. However, this may be accompanied by a reduction in fracture toughness due to the intensified melting and splashing effects. The optimal fracture toughness is often observed at moderate welding currents, such as 8 kA. Conversely, excessively high currents, like 16 kA, may yield minimal fracture toughness.

The duration of the welding process exerts a subtle yet discernible influence on the mechanical properties of the material, with prolonged welding times potentially leading to a reduction in fracture toughness, particularly in tensile shear joints. Nevertheless, the influence of welding time may differ depending on the specific joint configuration and welding parameters employed. The distribution of fracture toughness is influenced by electrode force, particularly in coach peel joints, where discrepancies in fracture toughness evolution have been observed across different electrode forces and welding currents. It has been demonstrated that lower electrode forces may yield higher fracture toughness at lower welding currents. However, the relationship between these variables is complex and may depend on specific joint characteristics. In conclusion, the observed trends highlight the critical importance of selecting optimal welding parameters to achieve the desired mechanical properties and performance in resistance spot welding joints. It is crucial to comprehend the relationship between welding current, welding time, and electrode force in order to achieve the optimal weld quality, penetration depth, and fracture toughness. The observed complexities in mechanical property evolution are attributed to variations in weld nugget formation and hardness within the boundary of the nugget and heat-affected zone. The current study offers valuable insights into the complex dynamics of resistance spot welding processes, providing guidance for practitioners to improve weld quality, mechanical integrity, and overall performance in a range of diverse welding applications.

ACKNOWLEDGMENT

This work has been supported by the Laboratory of mechanical systems and materials engineering: IS2M Tlemcen. The authors sincerely thank everyone who contributed to the preparation and finalization of this work.

REFERENCES

- [1] M. Vural and A. Akkus, "On the resistance spot weldability of galvanized interstitial free steel sheets with austenitic stainless steel sheets," *Journal of Materials Processing Technology*, vol. 153–154, pp. 1–6, Nov. 2004, <https://doi.org/10.1016/j.jmatprotec.2004.04.063>.
- [2] K. Vignesh, A. E. Perumal, and P. Velmurugan, "Optimization of resistance spot welding process parameters and microstructural examination for dissimilar welding of AISI 316L austenitic stainless steel and 2205 duplex stainless steel," *The International Journal of Advanced Manufacturing Technology*, vol. 93, no. 1, pp. 455–465, Oct. 2017, <https://doi.org/10.1007/s00170-017-0089-4>.
- [3] M. Ramdani, M. Benachour, and M. Rahou, "The Effects of Resistance Spot Welding Parameters on the Mechanical Behavior of Stainless Steel," *Engineering, Technology & Applied Science Research*, vol. 13, no. 2, pp. 10501–10504, Apr. 2023, <https://doi.org/10.48084/etasr.5019>.
- [4] T. Jagadeesha and T. J. S. Jothi, "Studies on the influence of process parameters on the AISI 316L resistance spot-welded specimens," *The International Journal of Advanced Manufacturing Technology*, vol. 93, no. 1, pp. 73–88, Oct. 2017, <https://doi.org/10.1007/s00170-015-7693-y>.
- [5] F. Ternane, M. Benachour, F. Sebaa, and N. Benachour, "Regression Modeling and Process Analysis of Resistance Spot Welding on

- Dissimilar Steel Sheets," *Engineering, Technology & Applied Science Research*, vol. 12, no. 4, pp. 8896–8900, Aug. 2022, <https://doi.org/10.48084/etasr.5059>.
- [6] F. Hayat and İ. Sevim, "The effect of welding parameters on fracture toughness of resistance spot-welded galvanized DP600 automotive steel sheets," *The International Journal of Advanced Manufacturing Technology*, vol. 58, no. 9, pp. 1043–1050, Feb. 2012, <https://doi.org/10.1007/s00170-011-3428-x>.
- [7] S. Zhang, "Stress Intensities at Spot Welds," *International Journal of Fracture*, vol. 88, no. 2, pp. 167–185, Nov. 1997, <https://doi.org/10.1023/A:1007461430066>.
- [8] L. P. Pook, "Fracture mechanics analysis of the fatigue behaviour of spot welds," *International Journal of Fracture*, vol. 11, no. 1, pp. 173–176, Feb. 1975, <https://doi.org/10.1007/BF00034726>.
- [9] L. P. Pook, "Approximate stress intensity factors obtained from simple plate bending theory," *Engineering Fracture Mechanics*, vol. 12, no. 4, pp. 505–522, Jan. 1979, [https://doi.org/10.1016/0013-7944\(79\)90093-6](https://doi.org/10.1016/0013-7944(79)90093-6).
- [10] D. Radaj and S. Zhang, "Simplified formulae for stress intensity factors of spot welds," *Engineering Fracture Mechanics*, vol. 40, no. 1, pp. 233–236, Jan. 1991, [https://doi.org/10.1016/0013-7944\(91\)90142-N](https://doi.org/10.1016/0013-7944(91)90142-N).
- [11] S.-H. Lin, J. Pan, P. Wung, and J. Chiang, "A fatigue crack growth model for spot welds under cyclic loading conditions," *International Journal of Fatigue*, vol. 28, no. 7, pp. 792–803, Jul. 2006, <https://doi.org/10.1016/j.ijfatigue.2005.08.003>.
- [12] P. Paris and F. Erdogan, "A Critical Analysis of Crack Propagation Laws," *Journal of Basic Engineering*, vol. 85, no. 4, pp. 528–533, Dec. 1963, <https://doi.org/10.1115/1.1365690>.
- [13] Z.-L. Lin and P.-C. Lin, "Geometric functions of stress intensity factor solutions for spot welds in coach-peel specimens," *Engineering Fracture Mechanics*, vol. 156, pp. 141–160, May 2016, <https://doi.org/10.1016/j.engfracmech.2016.01.023>.
- [14] S. Sedmak, I. Čamagić, A. Sedmak, Z. Burzić, and M. Arandelović, "The impact of the temperature and exploitation time on the tensile properties and plain strain fracture toughness, KIC in characteristic areas of welded joint," *Fratūra Ed Integrità Strutturale*, vol. 12, no. 46, pp. 371–382, Oct. 2018, <https://doi.org/10.3221/IGF-ESIS.46.34>.
- [15] M. Pouranvari, "Fracture toughness of martensitic stainless steel resistance spot welds," *Materials Science and Engineering: A*, vol. 680, pp. 97–107, Jan. 2017, <https://doi.org/10.1016/j.msea.2016.10.088>.
- [16] F. Krajcarz, A.-F. Gourgues-Lorenzon, E. Lucas, and A. Pineau, "Fracture toughness of the molten zone of resistance spot welds," *International Journal of Fracture*, vol. 181, no. 2, pp. 209–226, Jun. 2013, <https://doi.org/10.1007/s10704-013-9836-1>.
- [17] S. Zhang, "Approximate stress intensity factors and notch stresses for common spot-welded specimens," *Welding Journal*, vol. 78, no. 5, pp. 173–179, May 1999.
- [18] S. Zhang, "Stress Intensity Factors for Spot Welds Joining Sheets of Unequal Thickness," *International Journal of Fracture*, vol. 122, no. 1, pp. L119–L124, Jul. 2003, <https://doi.org/10.1023/B:FRAC.0000005406.06773.95>.
- [19] A. W. Society, *AWS C1. 1M/C1. 1-2000, Recommended Practices for Resistance Welding*, 4th ed. Miami, Florida: American Welding Society, 2000.
- [20] H. Tada, P. C. Paris, and G. R. Irwin, *The Stress Analysis of Cracks Handbook Third Edition*, 3rd. New York, NY, USA: ASME Press, 2000.
- [21] D. Radaj, "Stress singularity, notch stress and structural stress at spot-welded joints," *Engineering Fracture Mechanics*, vol. 34, no. 2, pp. 495–506, Jan. 1989, [https://doi.org/10.1016/0013-7944\(89\)90161-6](https://doi.org/10.1016/0013-7944(89)90161-6).
- [22] S. Zhang, "Fracture mechanics solutions to spot welds," *International Journal of Fracture*, vol. 112, no. 3, pp. 247–274, Dec. 2001, <https://doi.org/10.1023/A:1013588929709>.
- [23] S.-H. Lin, J. Pan, S.-R. Wu, T. Tyan, and P. Wung, "Failure loads of spot welds under combined opening and shear static loading conditions," *International Journal of Solids and Structures*, vol. 39, no. 1, pp. 19–39, Jan. 2002, [https://doi.org/10.1016/S0020-7683\(01\)00187-1](https://doi.org/10.1016/S0020-7683(01)00187-1).
- [24] D.-A. Wang, P.-C. Lin, and J. Pan, "Geometric functions of stress intensity factor solutions for spot welds in lap-shear specimens," *International Journal of Solids and Structures*, vol. 42, no. 24, pp. 6299–6318, Dec. 2005, <https://doi.org/10.1016/j.ijsolstr.2005.05.037>.
- [25] D.-A. Wang and J. Pan, "A computational study of local stress intensity factor solutions for kinked cracks near spot welds in lap-shear specimens," *International Journal of Solids and Structures*, vol. 42, no. 24, pp. 6277–6298, Dec. 2005, <https://doi.org/10.1016/j.ijsolstr.2005.05.036>.
- [26] P.-C. Lin, D.-A. Wang, and J. Pan, "Mode I stress intensity factor solutions for spot welds in lap-shear specimens," *International Journal of Solids and Structures*, vol. 44, no. 3, pp. 1013–1037, Feb. 2007, <https://doi.org/10.1016/j.ijsolstr.2006.05.031>.
- [27] P.-C. Lin and J. Pan, "Closed-form structural stress and stress intensity factor solutions for spot welds under various types of loading conditions," *International Journal of Solids and Structures*, vol. 45, no. 14, pp. 3996–4020, Jul. 2008, <https://doi.org/10.1016/j.ijsolstr.2008.02.006>.
- [28] P.-C. Lin and J. Pan, "Closed-form structural stress and stress intensity factor solutions for spot welds in commonly used specimens," *Engineering Fracture Mechanics*, vol. 75, pp. 5187–5206, Dec. 2008, <https://doi.org/10.1016/j.engfracmech.2008.08.005>.
- [29] M. R. A. Shawon, F. Gulshan, and A. S. W. Kurny, "Effect of Welding Current on the Structure and Properties of Resistance Spot Welded Dissimilar (Austenitic Stainless Steel and Low Carbon Steel) Metal Joints," *Journal of The Institution of Engineers (India): Series D*, vol. 96, no. 1, pp. 29–36, Apr. 2015, <https://doi.org/10.1007/s40033-014-0060-6>.
- [30] G. Janardhan, G. Mukhopadhyay, K. Kishore, and K. Dutta, "Resistance Spot Welding of Dissimilar Interstitial-Free and High-Strength Low-Alloy Steels," *Journal of Materials Engineering and Performance*, vol. 29, no. 5, pp. 3383–3394, May 2020, <https://doi.org/10.1007/s11665-020-04857-z>.
- [31] P. Peasura, "Effect of Electrode Force on Tensile Shear and Nugget Size of Austenitic Stainless Steel Grade 304 Welds Using Resistance Spot Welding," *Applied Mechanics and Materials*, vol. 52–54, Mar. 2011, <https://doi.org/10.4028/www.scientific.net/AMM.52-54.2176>.
- [32] M. Wohner, N. Mitzschke, and S. Jüttner, "Resistance spot welding with variable electrode force—development and benefit of a force profile to extend the weldability of 22MnB5+AS150," *Welding in the World*, vol. 65, no. 1, pp. 105–117, Jan. 2021, <https://doi.org/10.1007/s40194-020-01001-2>.
- [33] S. Salimi Beni, M. Atapour, M. R. Salmani, and R. Ashiri, "Resistance Spot Welding Metallurgy of Thin Sheets of Zinc-Coated Interstitial-Free Steel," *Metallurgical and Materials Transactions A*, vol. 50, no. 5, pp. 2218–2234, May 2019, <https://doi.org/10.1007/s11661-019-05146-8>.
- [34] I. Sevim, "Effect of hardness to fracture toughness for spot welded steel sheets," *Materials & Design*, vol. 27, no. 1, pp. 21–30, Jan. 2006, <https://doi.org/10.1016/j.matdes.2004.09.008>.